Journal of Functional Foods 109 (2023) 105797

Contents lists available at ScienceDirect

Journal of Functional Foods

journal homepage: www.elsevier.com/locate/jff

Attenuation of blue light-induced photo-oxidative stress through inhibition of NF-κB and MAPK signaling pathways, and activation of Nrf2 signaling pathway by djulis and its bioactive compounds

Ching-Chih Liu [a], Chin-Chen Chu [b], Shih-Ying Chen [c], Ying-Chun Lin [d], Pin-Der Duh [d,*]

[a] Department of Ophthalmology, Chi-Mei Medical Center, 710402, Taiwan, ROC
[b] Department of Anesthesiology, Chi-Mei Medical Center, 710402 Tainan, Taiwan, ROC
[c] Department of Health and Nutrition, Chia Nan University of Pharmacy and Science, Taiwan, ROC
[d] Department of Food Science and Technology, Chia Nan University of Pharmacy and Science, 60 Erh-Jen Road, Section 1, Pao-An, Jen-Te District, Tainan 71710, Taiwan, ROC

ARTICLE INFO

Keywords:
Djulis (*Chenopodium formosanum*)
Bioactive compounds
Blue light irradiation
Retinal pigment epithelium (RPE) cells
MAPK
Nrf2

ABSTRACT

The aim of this study is to investigate the djulis and its bioactive compounds to prevent blue light (BL)-induced photo-oxidative stress in ARPE-19 cells. After 6 h of BL exposure (peak at 452 nm), ARPE-19 cell viability significantly decreased, but treatment with water extract of djulis (WECF) at 0.1–25 μg/mL protected the cells from BL-induced phototoxicity. The cytoprotective effect of WECF were associated with a decrease in BL-induced oxidative stress and caspase-3 activity, and an increase in GSH levels and SOD activity. WECF also inhibited the expression of NF-κB protein and the MAPK signaling pathway, while upregulated heme oxygenase-1 (HO-1) via the Nrf2-mediated pathway. Moreover, betanin, kaempferol, quercetin and rutin, present in WECF, showed a protective effect against BL-induced photo-oxidative stress at 1–10 μM. Overall, WECF and its bioactive compounds have the potential to protect ARPE-19 cells from BL-induced retina damage, which could have therapeutic implications for retinal disease.

1. Introduction

Accumulating evidence shows that oxidative stress has been regarded as one of the important factors in human diseases due to its oxidizing effect on cellular DNA, protein and lipids (Yen, Chyau, Lee, Chu, Chang, & Duh, 2013). These diseases caused by oxidative stress affect human quality of life. For example, oxidative stress contributes to the development of age-related macular degeneration, a major and prevalent cause of blindness characterized in its initial stages by dysfunction, deterioration, and loss of the retinal pigment epithelium (RPE) in the macular area (Pocrnich, Liu, Feng, Peng, Feng, & Hutnik, 2009). Many studies have reported that light irradiation has both positive and negative effects on humans, animals and plants in nature. Blue light (BL) with short wavelengths between 400 and 480 nm helps regulate human circadian rhythm, or wake- and sleep cycle. However, in general, the shorter the wavelength, the higher the energy. That is to say that BL produces higher amount of energy. In addition, retinal pigment epithelial cells are vulnerable to oxidative damage as a result of excessive continual exposure to BL, which increases reactive oxygenes species (ROS) production in RPE cells. (Lu, Sun, Li, Sun, Yao, & Sun, 2016). Consequently, constant exposure of human to this type of light irradiation results in an increased risk of suffering from a variety of ocular disorders (Suárez-Barrio et al., 2020). Nowadays, people in modern developed society cannot avoid BL completely, therefore, many researches have been searching for effective solutions to prevent or reduce its damage to the eyes (Lu et al., 2016).

Many studies and epidemiological evidence show that increased dietary intake of bioactive compounds, such as phytochemicals, chemoprotective agents, and antioxidants, is associated with lower incidence of human diseases (Ness & Powles, 1997). In addition, early dietary intervention has been regarded as an effective, safer and feasible preventive strategy for prevention and treatment of photo-oxidative eye damage and RPE cell degeneration (Lu et al., 2016). Moreover, while BL causes oxidative stress in RPE cells, nuclear factor kappa-B (NF-κB) and mitogen-activated protein kinases (MAPK) have been recognized to be involved in oxidative stress-induced RPE degeneration (Kuse, Ogawa,

* Corresponding author.
E-mail address: ipdduh@mail.cnu.edu.tw (P.-D. Duh).

https://doi.org/10.1016/j.jff.2023.105797
Received 4 July 2023; Received in revised form 5 September 2023; Accepted 8 September 2023
Available online 22 September 2023

Tsuruma, Shimazawa, & Hara, 2014; Tsuchida & Sakiyama, 2023). Accumulating evidence shows that nuclear factor erythroid- derived 2-related factor (Nrf2), a transcription factor and master regulator of many antioxidant genes, deficiency in mice not only causes to age-related retinal degeneration, but also promotes RPE cell oxidative damage. There is some evidence that suggests the expression of naturally occurring bioactive compounds could be stimulated by the increased release of ROS to counteract oxidants and block their action, thereby reducing the oxidative damage caused by oxidation (Suárez-Barrio et al., 2020). In light of this, the research focused on the relationship between bioactive compound and MAPKs and Nrf2 signaling pathways, which may reduce oxidative damage to RPE cells, has attracted much attention in recent years, Therefore, a search for natural bioactive compounds which may attenuate photo-oxidative stress may be regarded as an effective and complementary therapeutic strategy for preventing and treating RPE dysfunction due to excessive BL exposure.

Djulis (*Chenopodium formosanum*) is a cereal plant rich in starch, protein, dietary fiber, valuable nutrients, minerals, grain-limited essential amino acids, and bioactive compounds (Hong, Huang, Lin, & Tsai, 2016). With respect to the biological activity of djulis, previous studies by the authors reported that djulis showed significant biological activities, including hepatoprotection (Chen, Chu, Chyau, Fu, & Duh, 2018), antiadipogenesis (Chyau, Chu, Chen, & Duh 2018), anti-hypertension (Chen, Chu, Chyan, Yang, & Duh, 2019), and inhibition of hyperlipidemia (Chen, Chu, Lin, & Duh, 2019). Djulis also showed to prevent colon carcinogenesis due to its antioxidant and apoptotic effect (Lee, Chen, Xie, & Shih, 2019). In addition, djulis protected human lung epithelial A549 cells from particulate matter (PM)-induced oxidative damage by up-regulating the expression of Nrf2 and HO-1 via the ERK and JNK signaling pathways (Chu, Chen, Chyau, Wang, Chu, & Duh, 2022). In particular, the bioactive compounds present in djulis, such as betanin, rutin, kaempferal, quercetin, and other compounds, may partly account for its multibiological effects (Chu et al., 2022). Despite these remarkable biological activities, it remains unclear whether djulis has the function of protecting the retina from oxidative damage caused by BL exposure. Therefore, this *in vitro* study aims to investigate the effects of djulis and its bioactive compounds on regulating BL-induced photo-oxidative damage in RPE cells and to elucidate the antioxidant pathways involved.

2. Materials and methods

2.1. Materials

3-(4,5-dimethylthiazol-2-yl)-2,5-diphenyltetrazolium bromide (MTT) were purchased from Sigma-Aldrich Chemical Co. (St. Louis, MO, USA). Nrf2 antibody, HO-1 antibody and Lamin B1 antibody were purchased from Affinity Biosciences, (Cincinnati, OH, USA). Quercetin (≥95% purity) was obtained from Sigma-Aldrich (St. Louis, MO, USA). Kaempferol (≥99% purity) was purchased from Indofine Chemical Company Inc. (Hillsborough, NJ., USA). Betanin (red beet extract diluted with dextrin) was supplied from Tokyo Chemical Industry Co., Ltd. (Tokyo, Japan). Rutin (≥97% purity) was bought from Alfa Aesar (Haverhill, MA, USA). ARPE-19 cells were purchased from the Bioresource Collection and Research Center (BCRC, Food Industry Research and Development Institute, Hsinchu, Taiwan). The chemicals used in the research were analytical grade.

2.2. WECF preparation

The djulis (*Chenopodium formosanum*) was obtained from Colaidea Co., Ltd., Pingtung, Taiwan. Djulis, which was identified by Professor Yau-Lun Kuo of the Department of Forestry, National Pingtung University of Science and Technology, Pingtung, Taiwan, ~~was purchased from Kullku Farm (Pingtung, Taiwan)~~ and ground to a fine powder using a high speed grinder (RT08, Rong Tsong, Taipei, Taiwan) prior to extraction. The voucher specimen (No. CNU-101) was deposited in the Department of Food Science and Technology, Chia Nan University of Pharmacy and Science, Tainan, Taiwan. Djulis was extracted with boiling water at the ratio of 1:10 (w/v) for 20 min. After filtering through Advantec No.2 filter paper (Toyo Roshi Kaisha, Ltd., Tokyo, Japan), the residue was re-extracted under the same conditions. The supernatants were combined and concentrated using a rotary evaporator under reduced pressure and then freeze-dried. The resulting water extracts of djulis, abbreviated as WECF, were stored at −20℃ until use.

2.3. Blue light irradiation

Blue light emitting diodes (LEDs) with a peak at 452 nm and an intensity of 1680 lx were used for light delivery (T5CLED1-BLUE 8 W, Zoomlighting, Taiwan). The light intensity was measured with a LX-103 light meter (Lutron, Taiwan) and the average height of the LED was 50 mm above the bottom of each culture. The samples were maintained at room temperature during irradiation.

2.4. Cell culture and cell viability assay

ARPE-19 cells were cultured in 90% Ham's F12K medium supplemented with 10% (v/v) fetal bovine serum and 2 mM L-glutamine at 37 °C in a humidified atmosphere containing 5% CO_2. The viability of ARPE-19 cells was determined by MTT assay. Cells were seeded in 96-well plates at a density of 2×10^4 cells/well and incubated for 24 h. After irradiation with blue light for 6 h at a distance of 50 mm from the LED, WECF at 0.1–25 μg/mL and bioactive compounds at 1–10 μM were added to the medium and incubated at 37 °C for 18 h. Then, 50 μL of 0.1% MTT was added in each well and incubated at 37 °C for 2 h. The medium was subsequently removed, and *l*00 μl of dimethyl sulfoxide (DMSO) was added to dissolve the colored formazan crystal and measured at 540 nm using an ELISA reader (Molecular Devices VMax, Visalia, CA, USA) (Chyau, Chu, Chen, & Duh, 2015).

2.5. Determination of intracellular reactive oxygen species

In order to detect intracellular reactive oxygen species (ROS), DCFH-DA (2′,7′-dichlorofluorescin diacetate) was used as a probe. ARPE-19 cells were seeded in 6-well plates at a density of 4×10^5 cells/well and incubated for 24 h. After the cells were exposed to blue light, as indicated, at a distance of 50 mm to the LED, for 0.5 h, the cells were treated with WECF (0.1–25 μg/mL) and bioactive compounds at concentrations of 1, 5, 10 μM, and incubated with 50 μM DCFH-DA at 37 °C for 1 h. Following incubation, the fluorescence intensity was measured using a Bio-Tek FLx 800 microplate fluorescence reader (excitation wavelength: 485 nm; emission wavelength: 528 nm), and the intracellular ROS produced as a result of stress was expressed as the percentage of fluorescence intensity relative to the negative control (Wang, and Joseph, 1999).

2.6. Determination of intracellular lipid peroxidation

Malondialdehyde (MDA) is a final product and used as a biomarker for lipid peroxidation. The measurement of MDA was based on a reaction with thiobarbituric acid (TBA) to generate a product, thiobarbituric acid-reactive substances (TBARS), which could be detected fluorimetrically. ARPE-19 cells were seeded in 6-well plates at a density of 4×10^5 cells/well and incubated for 24 h. After the cells were exposed to blue light, as indicated, at a distance of 50 mm to the LED for 4 h, the cells were treated with WECF (0.1–25 μg/mL) and bioactive compounds at concentrations of 1, 5, 10 μM, and incubated at 37 °C for 1 h. After incubation, 1 mM butylated hydroxyanisole (BHA) was added, the reaction solution was extracted and mixed with trichloroacetic acid (TCA) and TBA for 10 min in boiling water. The fluorescence intensity was measured using a Bio-Tek FLx 800 microplate fluorescence reader (excitation wavelength: 530 nm; emission wavelength: 560 nm) (Chirico, Smith, Marchant, Mitchinson, & Halliwel, 1993).

2.7. Determination of intracellular glutathioine (GSH)

To detect intracellular glutathione, a fluorescent dye called CMF-DA (5-chloromethylfluorescein diacetate) was used. This dye can pass through cell membranes for detection of glutathione. ARPE-19 cells were seeded in 6-well plates at a density of 4 × 10^5 cells/well and incubated for 24 h. After the cells were irradiated with blue light, as indicated at a distance of 50 mm to the LED, for 0.5 h, the cells were treated with WECF (0.1–25 μg/mL) and bioactive compounds at concentrations of 1, 5, 10 μM, and incubated at 37 °C for 1 h. Following incubation, cells were washed with PBS and treated with 5 μM CMF-DA for 30 min. The cells were then washed again with PBS, and the intracellular GSH was measured using a Bio-Tek FLx 800 microplate fluorescence reader (excitation wavelength: 485 nm; emission wavelength: 528 nm) (Wu, Huang, Lian, Kou, Wang, 2005).

2.8. Evaluation of superoxide dismutase (SOD)

SOD activity was determined using the Sigma-Aldrich SOD assay kit (Cayman Chemical, Ann Arbor, MI, USA) according to the manufacture's protocol. In brief, ARPE-19 cells were seeded in a 6-well plate at a density of 5 × 10^5 cells/dish and incubated for 24 h. After the cells were irradiated with blue light as indicated, at a distance of 50 mm to the LED, for 0.5 h, the cells were treated with WECF (0.1–25 μg/mL) and 1, 5, 10 μM bioactive compounds, and incubated at 37 °C for 4 h. The sample and each reagent (No. 1, 2, 3, and 4) were mixed thoroughly and the optical density was measured at 450 nm using a microplate spectrophotometer (Thermo Multiskan GO, Waltham, MA, USA) after incubation for 20 min at 37 °C.

2.9. Measurement of mitochondrial membrane potential (ΔΨm)

The mitochondrial membrane potential of cells was determined using the JC-1 mitochondrial membrane potential assay kit (Cayman Chemical Company, Ann Arbor, MI, USA). The cells were seeded at a density of 2.0 × 10^5 cells/mL in 6 well plates and incubated for 24 h. After irradiating the cells with blue light for 3 h at a distance of 50 mm from the LED, they were treated with WECF (0.1–25 μg/mL) and incubated at 37 °C for 15 min. Then, JC-1 was added to the cells and incubated at 37 °C for 30 min in a humidified 5% CO_2 incubator. The cells were collected, washed with 200 μL of PBS, and centrifuged (75.53 g, at 4 ℃, 5 min). They were suspended in 100 μL of PBS and analyzed using a fluorophotometer (FLx 800, BioTek, Winooski, VT, USA) with an excitation wavelength of 530 nm and an emission wavelength of 590 nm to measure fluorescence.

2.10. Determination of caspase-3 activity

Caspase-3 activity was determined using the BioVision CPP32/Caspase-3 colorimetric assay kit (Milpitas, CA, USA). In brief, ARPE-19 cells were seeded on a 10 cm dish (3 × 10^6 cells/dish) and cultured for 24 h. After irradiating the cells with blue light for 4 h at a distance of 50 mm to the LED, as indicated, the cells were treated with WECF (0.1–25 μg/mL) and 1, 5, 10 μM bioactive compounds, and incubated at 37 °C for 2 h. After incubation, the cells were washed with cold PBS, treated with 1 mL trypsin-EDTA for 3 min, and suspended in PBS after centrifugation. Cell lysates were pelleted, followed by transfer of the supernatants to microcentrifuge tubes. To each tube, 50 μL of reaction buffer with 5 mmol/DTT and 5 μLof 1 mmol/l DEVD-p-nitroanilide (pNA)-conjugated CPP32 substrate were added, followed by 1 h incubation in a water bath at 37 °C. Optical density (OD) for each specimen was determined at 405 nm using an ELISA reader (Molecular Devices VMax, MA, USA) (Chyau, Chu, Chen, & Duh, 2015).

2.11. DAPI staining assay

ARPE-19 cells were seeded on a 6-well (5 × 10^5 cells/well) and cultured for 24 h. After irradiating the cells with blue light for 4 h at a distance of 50 mm to the LED, as indicated, the cells were treated with WECF (0.1–25 μg/mL) and 10 μM bioactive compounds, and incubated at 37 ℃ for 2 h. After incubation, ARPE-19 cells were washed with PBS, and fixed with 4% paraformaldehyde in PBS for 30 min. Fixed cells were washed with PBS and stained with DAPI (4′,6′-diamidino-2-phenylindole). Evaluation was performed using a fluorescence microscope with a 350 nm excitation and a 461 nm filter for detection (Duh, Chen, Lee, Lin, Wang, Yen, Kuo, & Chu, 2012).

2.12. Western blot analysis

Western blots were performed as previously described (Chyau, Chu, Chen, & Duh, 2015) with some modifications. In brief, ARPE-19 cells were seeded on a 10 cm dish (2 × 10^6 cells/dish) and cultured for 24 h. After the cells were irradiated with blue light as indicated, at a distance of 50 mm to the LED, for 6, 0.5, 2, and 3 h to determine NF-κB, MAPKs (ERK, JNK and p38), Nrf2 and HO-1, the cells were treated with WECF (0.1–25 μg/mL) and 1, 5, 10 μM bioactive compounds and incubated at 37 ℃ for 15, 2, 14 and 16 h to determine NF-κB, MAPKs (ERK, JNK and p38), Nrf2 and HO-1, respectively. The cells were washed with ice-cold phosphate buffer saline (PBS), and then the cells were treated with lysis buffer. Cellular lysates were centrifuged at 10,000 xg at 4 ℃ for 10 min. The supernatants were collected, and the protein contents were determined using the BCA protein assay kit (Piece, Pockfold, IL, USA). Each sample, containing 50 μg protein, was separated on 8% or 12% sodium dodecyl sulfate SDS–polyacrylamide gels. After electrophoresis, gels were transferred to a nitrocellulose membrane. After washing with distilled water, the membrane was incubated with 5% albumin in PBST (0.1% Tween-20 in PBS, pH 7.4) for 30 min and then immunoblotted with rabbit monoclonal anti-NF-κB antibody (#8242) (1:1000) (Cell Signaling Technology, Danvers, MA, USA), rabbit anti-JNK (AF6318) (1:1000), rabbit anti-pJNK (AF3319) (1:1000), rabbit pp38 (AF4001) (1:1000), rabbit anti-p38 (AF6456) (1:1000), rabbit anti-ERK (AF0155) (1:1000), rabbit pERK (AF1015) (1:1000), anti-Nrf2 (AF0639) (1:1000), anti-HO-1 (DF6391) (1:1000), anti-Lamin B1 (AF5161) (1:1000) (Affinity Biosciences, Cincinnati, OH, USA), and β-actin antibody (#4970) (1:1000) (Cell Signaling Technology, Danvers, MA, USA) overnight at 4 ℃. Blots were then incubated with anti-rabbit immunoglobulin G (IgG) antibody conjugated to horseradish peroxidase (Sigma, St. Louis, MO, USA). Blots were developed using the Western Bright Enhanced Chemiluminescence (ECL) plus kit (Advansta Inc., Menlo Park, CA, USA), exposed to Gel Electrophoresis Documentation-Multifunction Gel Image system (Topbio Co., Taiwan, ROC). The relative expression of proteins was quantified densitometrically using the Image J software and calculated according to the reference bands of β-actin.

2.13. Statistical analysis

Each experiment was performed at least triplicate and averaged. Data are expressed as mean ± SD, and ANOVA was conducted by using the SPSS software (version 12.0, SPSS Inc., Chicago, IL, USA). When a significant F ratio was obtained ($p < 0.05$), a post hoc analysis was conducted between groups by using a Duncan's multiple range tests. A significant difference between treatments was considered when *p*-values<0.05.

3. Results

3.1. ARPE-19 cell survival

Fig. 1 depicts the effects of WECF on BL-induced ARPE-19 cell viability. Fig. 1A shows the effect of BL irradiation on ARPE-19 cell

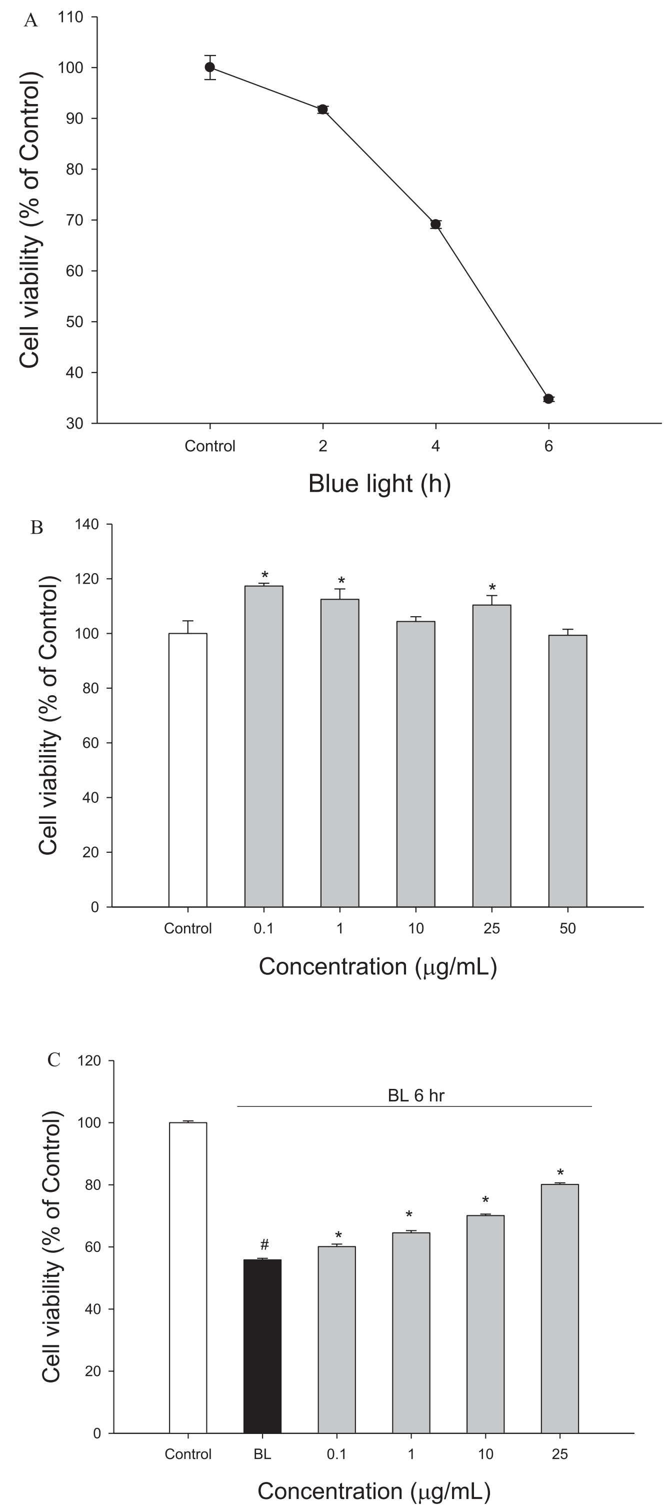

Fig. 1. Effects of water extracts of djulis (WECF) on ARPE-19 cell viability induced by blue light (BL) exposure. (A) Effect of blue light exposure duration on ARPE-19 cell viability. The cells were incubated for 18 h. (B) Effects of different concentrations of WECF on ARPE-19 cell viability. The cells were treated with WECF for 24 h. (C) Effects of water extracts of djulis (WECF) on BL-induced ARPE-19 cell viability. The cells were exposed to blue light for 6 h and then treated with WECF for 18 h. $^{\#}$($p < 0.05$) compared to the control group, and *($p < 0.05$) compared to blue light (BL)-induced cells alone. Data are presented by means ± SD (n = 3).

viability. After irradiation with blue light for different times, WECF at concentrations ranging from 0.1 to 25 μg/mL were added to the medium and incubated at 37 °C for 18 h. The cell survival was then determined using the MTT assay. BL irradiation for 2, 4 and 6 h resulted in a decrease in ARPE-119 cell survival to 91.7 ± 0.7, 69.1 ± 0.7, and 34.7 ± 0.4%, respectively. Clearly, BL irradiation for 6 h reduced cell viability by approximately 66% in comparison to the control. Moreover, WECF at doses ≤ 25 μg/mL did not significantly affect the cell viability as compared with the control (Fig. 1B), indicating that WECF under the tested doses is not toxic to ARPE-19 cells. To investigate the protective effect of WECF against BL-induced cell damage, ARPE-19 cells were incubated with WECF after BL exposure showed a dose-dependent increase in cell viability compared to cells exposed to BL alone (Fig. 1C). These findings suggest that BL decreases ARPE-19 cell viability, and this is attenuated with WECF treatment in a dose-dependent manner. Consequently, cells treated with WECF after BL exposure for 6 h and doses of<25 μg/mL were chosen for further experiments.

3.2. WECF reduced photo-oxidation and restored antioxidant indices

Fig. 2 demonstrates that WECF reduced photo-oxidation and restored antioxidant indices in BL-induced ARPE-19 cells. To investigate the effect of WECF on photo-oxidation in BL-induced ARPE-19 cells, ROS production was measured after BL irradiation. As illustrated in Fig. 2A, BL irradiation significantly enhanced ROS production by 172.7 ± 5.1% in comparison to the control (100%). Interestingly, treatment of ARPE-19 cells with WECF ranging from 0.1 to 25 μg/mL significantly reduced ROS production in BL irradiation to values, which were intermediate between those of the control and BL-induced cells. It was apparent that BL irradiation significantly induced cells photo-oxidation. However, the tested doses of WECF offered a significant inhibitory effect on photo-oxidation of ARPE-19 cells induced by BL irradiation. The protective effect of WECF on lipid peroxidation in BL-induced ARPE-19 cells was determined (Fig. 2B). The treatment of ARPE-19 cells with BL irradiation for 4 h resulted in as increase in TBARS formation, indicating that BL triggered ARPE-19 cell photo-oxidation. As expected, when cells were incubated with WECF ranging from 0.1 to 25 μg/mL after exposure to BL irradiation, TBARS formation significantly decreased. No significant difference ($p > 0.05$) was found between WECF at 25 μg/mL and the control in inhibiting effect on TBARS formation.

To assess the impact of WECF on antioxidant indices in BL-induced ARPE-19 cells, the enzymatic and nonenzymatic antioxidant indices were analyzed. Fig. 2C illustrates the effect of WECF on reduced GSH levels in ARPE-19 cells induced by BL irradiation. The results indicated that exposure of cells to BL irradiation for 0.5 h led to a significant decrease GSH levels (69.2 ± 2.5%) compared to the control. However, the decrease in GSH levels induced by BL irradiation was significantly alleviated by WECF. Additionally, the study also examined the activity of SOD, a well-known enzymatic antioxidant. The SOD activity was significant lower in BL-induced ARPE-19 cells (7.1 ± 0.4 U/mg protein) than in the control (13.4 ± 0.4 U/mg protein) (Fig. 2D). The SOD activity in cells treated with WECF at doses ≤ 25 μg/mL increased in a dose-dependent manner. Specifically, the SOD activity of ARPE-19 cells treated with WECF at 25 μg/mL was 15.0 ± 0.9 U/mg protein, and no significant difference was found between WECF and the control regarding their on restorative effect on SOD activity in BL-inducing ARPE-19 cells.

3.3. Effect on mitochondrial membrane potential, caspase-3 activity and DAPI staining

To obtain more information about the involvement of WECF in the inhibiting the apoptosis process in BL induced ARPE-19 cells, the study evaluated the effects of WECF on mitochondrial membrane potential, caspase-3 activity and DAPI staining (Fig. 3). The results showed that exposure of cells to BL for 3 h led to a dramatic decrease in

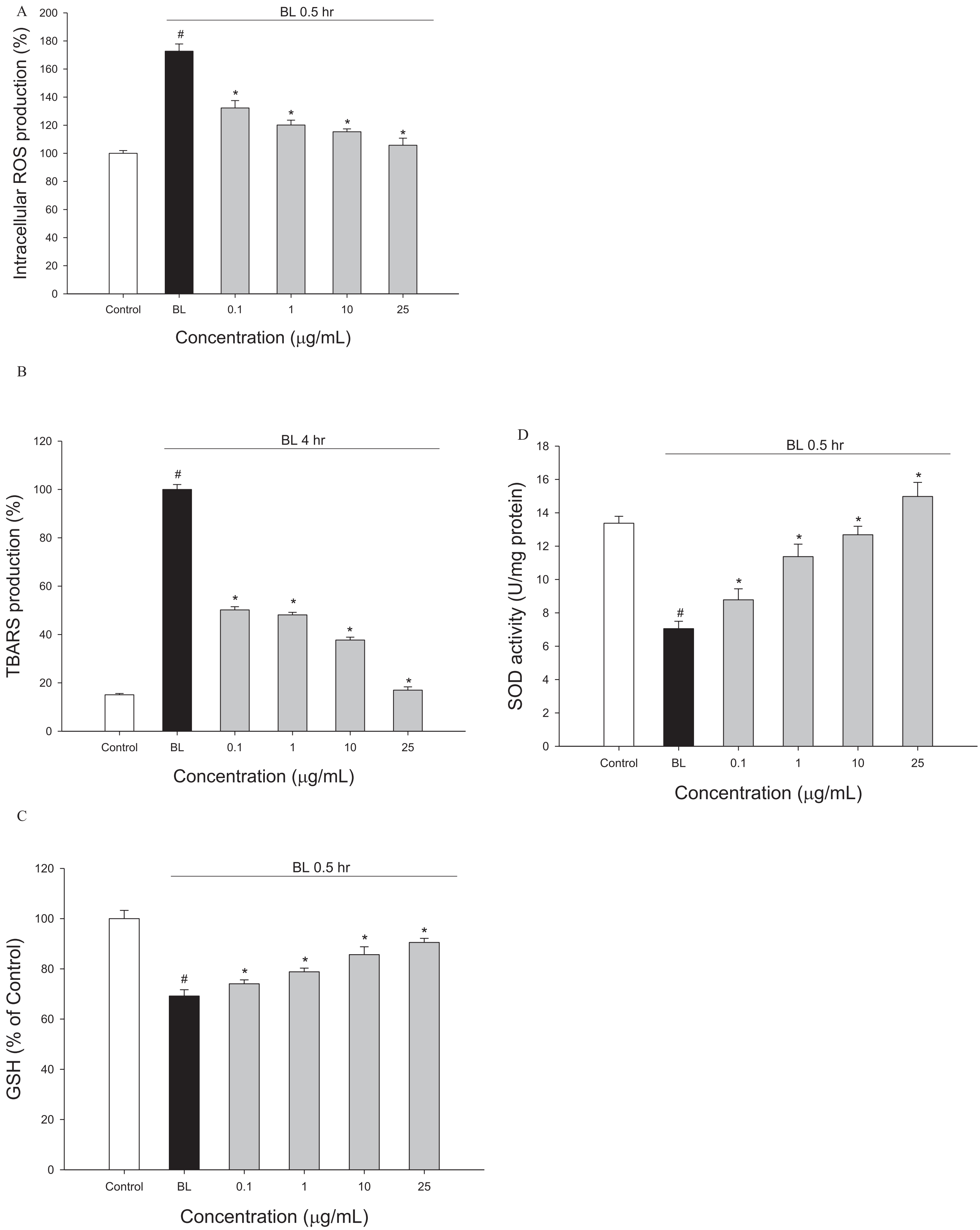

Fig. 2. Effects of water extracts of djulis (WECF) on blue light (BL)-induced oxidation and antioxidant indices in ARPE-19 cells. (A) Effects of WECF on blue light (BL)-induced intercellular ROS production in ARPE-19 cells. The cells were exposed to blue light for 0.5 h and then treated with WECF for 1 h. (B) Effects of WECF on blue light (BL)-induced intercellular TBARS formation in ARPE-19 cells. The cells were exposed to blue light for 4 h and then treated with WECF for 1 h. (C) Effects of WECF on blue light (BL)-induced glutathione (GSH) contents in ARPE-19 cells. The cells were exposed to blue light for 0.5 h and then treated with WECF for 1 h. (D) Effects of WECF on blue light (BL)-induced SOD activity in ARPE-19 cells. The cells were exposed to blue light for 0.5 h and then treated with WECF for 4 h. #($p < 0.05$) compared to the control group, and *($p < 0.05$) compared to blue light (BL)-induced cells alone. Data are presented by means ± SD (n = 3).

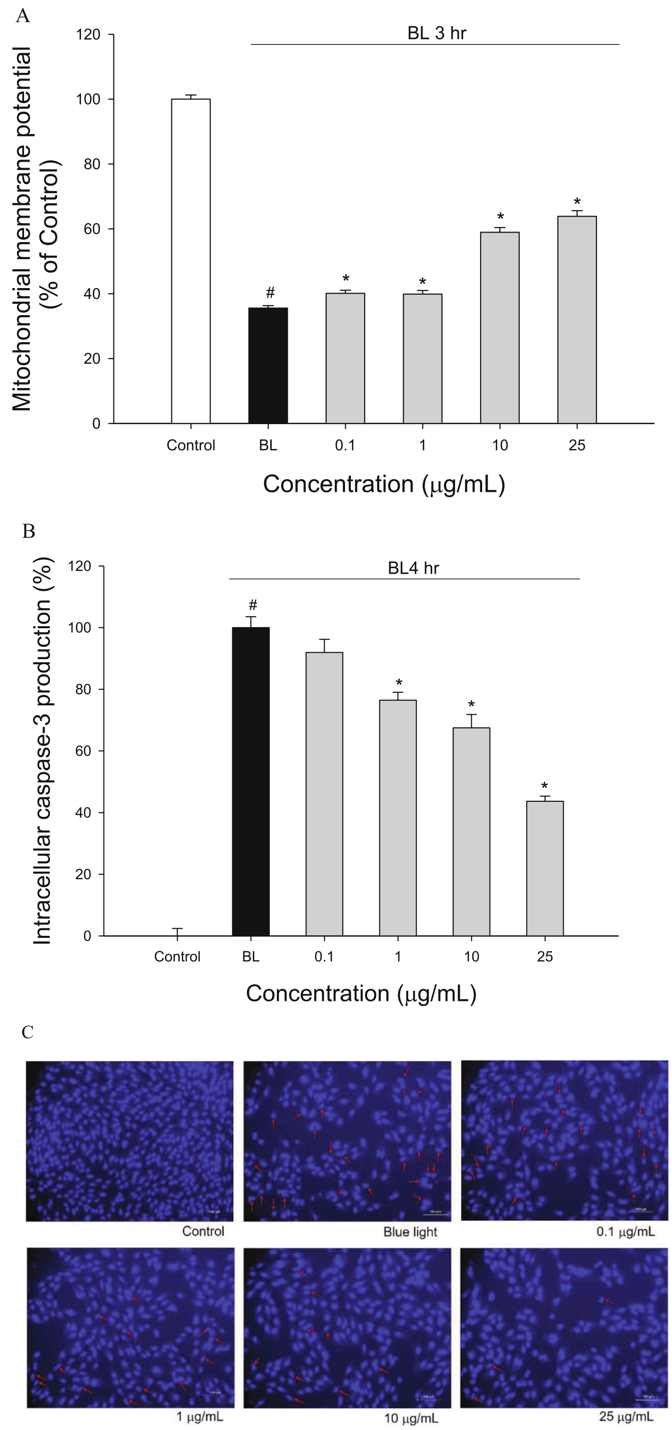

Fig. 3. Effects of WECF on mitochondrial membrane potential (A), caspase-3 activity (B), and DAPI staining (C) in blue light (BL)-induced ARPE-19 cells. The cells were exposed to blue light for 3 h (A), 4 h(B) and 4 h(C) and then treated with WECF for 15 min (A), 2 h(B) and 2 h(C), respectively. The arrows demonstrated shrinkage and rounding of apoptotic cells. $^{\#}(p < 0.05)$ compared to the control group, and $^{*}(p < 0.05)$ compared to blue light (BL)-induced cells alone. Data are presented by means ± SD (n = 3).

mitochondrial membrane potential indicating that BL induced mitochondial damage. However, treatment of cells with WECF at 10 and 25 μg/mL significantly protected the cells against the decrease in mitochondrial membrane potential induced by BL (Fig. 3A). The study also investigated the effect of WECF on caspase-3 activity to determine its involvement in inhibiting the apoptosis process. The results indicating that caspase-3 activity in cells treated with BL irradiation for 4 h increased significantly compared to the control (Fig. 3B). However, the results showed that WECF dose-dependently reduced the activity of caspase-3 in BL-induced cells. Therefore, WECF appear to suppress caspase-3 activity in BL-induced cell photo-oxidation, leading to a reduction in the apoptosis process in BL induced ARPE-19 cells. Moreover, DAPI staining was conducted to investigate the morphological changes of the nuclei of ARPE-19 cells induced by BL. The results indicated that while normal cells displayed round and stained uniformly dispersed chromatin and intact cell membranes in the control group, the cells exposed to BL for 4 h exhibited condensed and fragmented nuclei, indicative of apoptosis (Fig. 3C). However, cells treated with different concentrations of WECF showed reduced fragmentation in the chromatin and DNA rings within the cell nucleus, indicating an anti-apoptotic effect. These observations suggest that WECF exhibited a dose-dependent anti-apoptotic effect on LB-induced ARPE-19 cells.

3.4. *Effect of WECF on NF-κB and MAPKs signaling pathways in BL induced ARPE-19 cells*

To investigate the molecular mechanisms underlying the protective effect of WECF against BL-induced photo-toxicity, the study examined the regulating effects of WECF on the NF-κB and MAPKs signaling pathways. Fig. 4 shows the effect of WECF on NF-κB and MAPKs signaling pathways in BL induced ARPE-19 cells. NF-κB is a transcription factor that regulates innate immunity and contributes to overall mitochondrial function. Therefore, the effect of WECF on NF-κB in blue light-induced ARPE-19 cells was determined. As depicted in Fig. 4A, the nuclear protein level of NF-κB increased by 4.84-fold in the BL-induced group compared to the control group. However, WECF treatment at 25 μg/mL demonstrated comparatively strong inhibitory effects on nuclear protein level of NF-κB in treated cells, suggesting that WECF treatment inhibits NF-κB translocation, prevents the BL-induced nuclear transcriptional level of NF-κB in in BL-induced ARPE-19 cells (Fig. 4A).

To gain the insights into molecular mechanisms of WECF, the phosphorylation of JNK, ERK, and p38 MAPK in BL-induced ARPE-19 cells was further investigated. Fig. 4B depicts the effects of WECF on MAPKs signaling pathways in BL-induced ARPE-19 cells. Blue light treatment significantly induced the phosphorylation of ERK, JNK, and p38 (1.49-, 1.43-, and 1.22-fold, respectively) compared to the control, indicating the activation of ERK, JNK, and p38 MAPK. However, WECF at 25 μg/mL effectively inhibited the phosphorylation of ERK, JNK, and p-38 by 28.9%, 48.3%, and 33.6%, respectively, relative to BL alone group. These results suggest that WECF prevents the phosphorylation of ERK, JNK, and p38 induced by BL treatment. Therefore, the inhibitory effects of WECF on BL-induced cell photo-oxidative damage may be related to a concomitant inhibition of JNK, ERK, and p38 MAPK signaling in BL-induced ARPE-19 cells.

3.5. *Effect of WECF on Nrf2 protein expression and HO-1 activity*

It is widely known that oxidative stress increases Nrf2 protein expression. As BL irradiation induces ROS production, we further investigated whether BL-induced photo-oxidation also activated the Nrf2 pathway, and if the Nrf2 protein expression in BL-induced cells was affected by WECF treatment. Fig. 5 shows the effect of WECF (at 25 μg/mL) on Nrf2 protein expression and HO-1 activity. Nrf2 is known to be an emerging regulator of intracellular resistance of oxidative stress, so the effect of WECF on Keap1-Nrf2 pathway induced by BL irradiation was further investigated. Specifically, in terms of protein expression, we further analyzed Nrf2 protein expression in cytoplasm and nucleus. As shown in Figurer 5A, Nrf2 protein expression in the cytoplasm decreased in the presence of BL irradiation compared to the control group and WECF group. However, the Nrf2 proton expression in the nucleus was higher in the presence of WECF compared to both the control group and BL irradiation. These findings suggest that WECF enhanced the nuclear

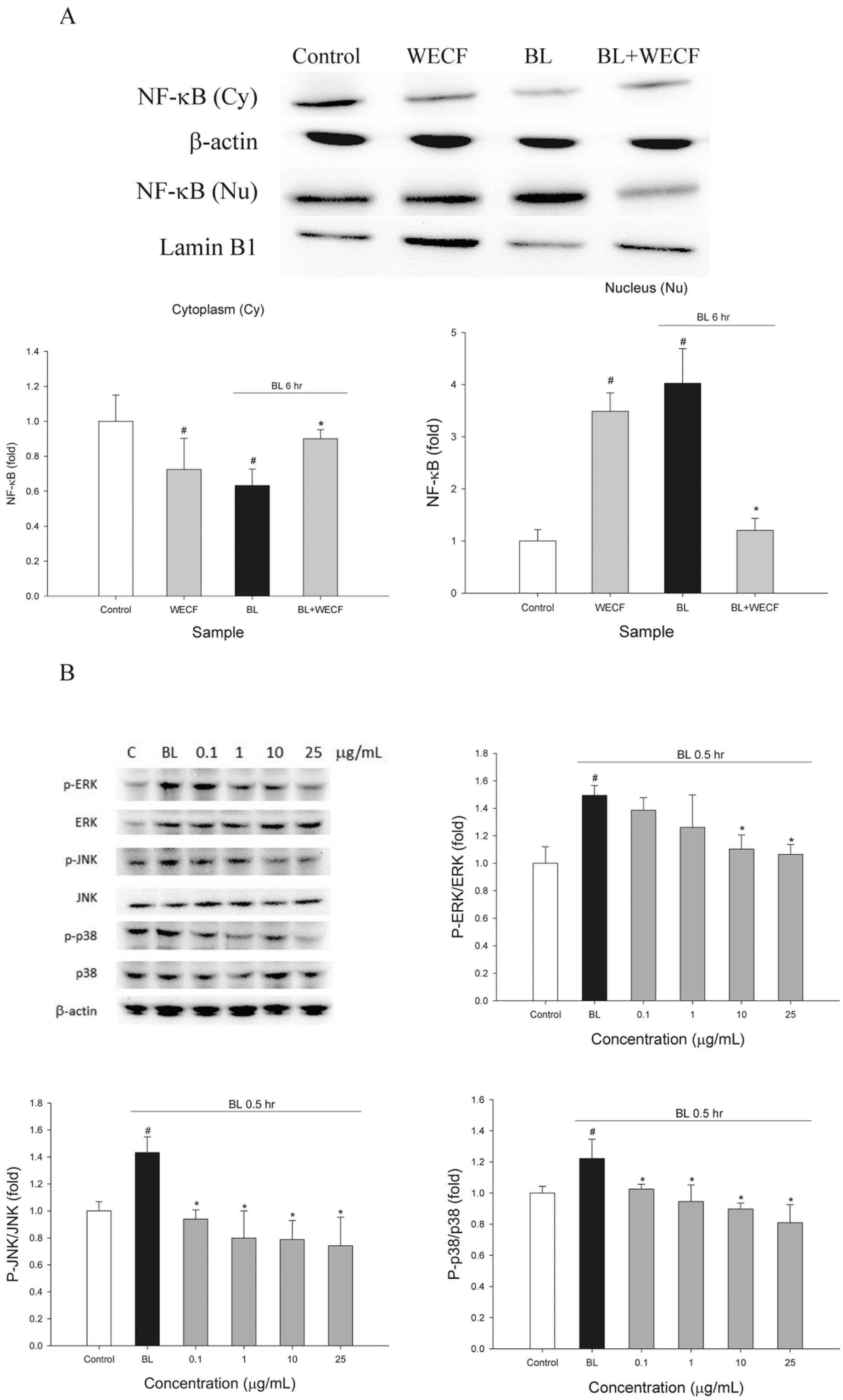

Fig. 4. Effects of water extracts of djulis (WECF) on NF-kB and MAPKs signaling pathways in blue light (BL)-induced ARPE-19 cells. (A) Effects of WECF on blue light (BL)-induced NF-kB signaling pathways in ARPE-19 cells. The cells were exposed to blue light for 6 h and then treated with WECF for 15 h. (B) Effects of WECF on blue light (BL)-induced on ERK, JNK and p38 signaling pathways in ARPE-19 cells. The cells were exposed to blue light for 0.5 h and then treated with WECF for 2 h. $^{\#}$($p < 0.05$) compared to the control group, and *($p < 0.05$) compared to blue light (BL)-induced cells alone. Data are presented by means ± SD (n = 3).

Nrf2 protein expression in BL-induced cells. Fig. 5B shows the expression of heme oxygenase-1 (HO-1), which increased under BL irradiation as compared to the control group. The results showed that HO-1 gene expression was induced by the presence of BL irradiation as well as in the group where WECF was combined with BL irradiation. These results confirmed that WECF stimulated the expression of HO-1 in BL-induced ARPE-19 cells.

3.6. Bioactive compounds present in WECF protect ARPE-19 cells from BL induced-photo-oxidation

The effects of bioactive compounds found in WECF, such as betanin, rutin, kaempferol and quercetin, on cell growth of ARPE-19 cells and their antioxidant indices after BL-induced damage were determined (Fig. 6). The results showed that treatment of ARPE-19 cells with betanin, rutin, kaempferol and quercetin at 5 and 10 μM after BL exposure significantly increased cell viability compared to BL alone (Fig. 6A).

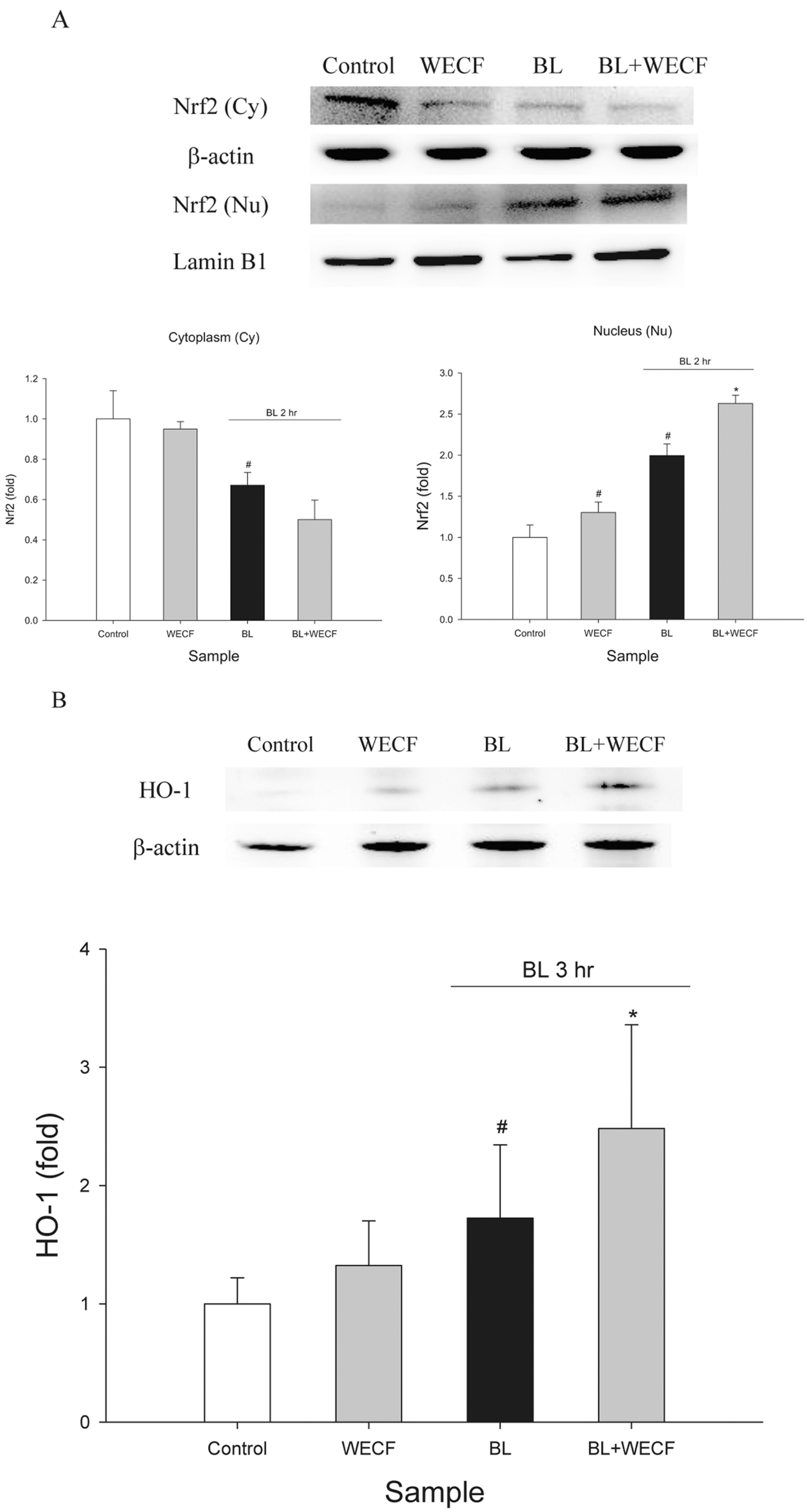

Fig. 5. Effects of water extracts of djulis (WECF) on Nrf2 and HO-1 protein expression in blue light (BL)-induced ARPE-19 cells. (A) Effects of WECF on blue light(BL)-induced expression of Nrf2 in ARPE-19 cells. The cells were exposed to blue light for 2 h and then treated with WECF (25 μg/mL) for 14 h. (B) Effects of WECF on blue light(BL)-induced HO-1 activity in ARPE-19 cells. The cells were exposed to blue light for 3 h and then treated with WECF (25 μg/mL) for 16 h. $^{\#}$($p < 0.05$) compared to the control group, and *($p < 0.05$) compared to blue light (BL)-induced cells alone. Data are presented by means ± SD (n = 3).

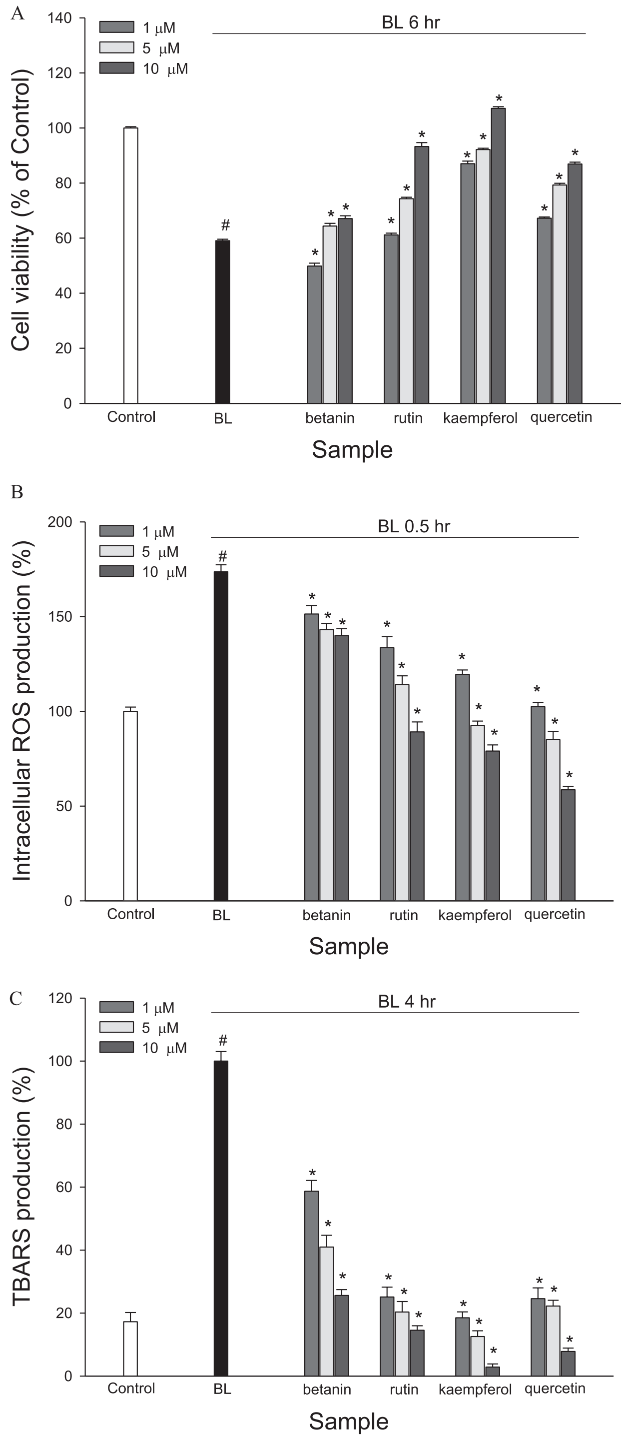

Fig. 6. Effects of betanin, rutin, quercetin, and kaempferol on cell viability, oxidation, antioxidant indices, Nrf2 protein expression and HO-1 protein levels in blue light (BL)-induced ARPE-19 cells. (A) Effects of betanin, rutin, quercetin, and kaempferol on blue light (BL)-induced ARPE-19 viability. The cells were exposed to blue light for 6 h and then treated with bioactive compounds for 18 h. (B) Effects of betanin, rutin, quercetin, and kaempferol on blue light (BL)-induced intercellular ROS production in ARPE-19 cells. The cells were exposed to blue light for 0.5 h and then treated with bioactive compounds for 1 h. (C). Effects of betanin, rutin, quercetin, and kaempferol on blue light (BL)-induced intercellular TBARS formation in ARPE-19 cells. The cells were exposed to blue light for 4 h and then treated with bioactive compiunds for 1 h. (D) Effects of betanin, rutin, quercetin, and kaempferol on blue light (BL)-induced glutathione (GSH) contents in ARPE-19 cells. The cells were exposed to blue light for 0.5 h and then treated with bioactive compounds for 1 h. (E) Effects of betanin, rutin, quercetin, and kaempferol on blue light (BL)-induced SOD activity in ARPE-19 cells. The cells were exposed to blue light for 0.5 h and then treated with bioactive compounds for 4 h. (F) Effects of betanin, rutin, quercetin, and kaempferol on blue light (BL)-induced expression of Nrf2 in ARPE-19 cells. The cells were exposed to blue light for 2 h and then treated with bioactive compounds (10 μM) for 14 h. B, betanin; R, rutin; Q, quercetin; K, kaempferol. (G) Effects of betanin, rutin, quercetin, and kaempferol on blue light (BL)-induced HO-1 activity in ARPE-19 cells. The cells were exposed to blue light for 3 h and then treated with bioactive compounds (10 μM) for 16 h. B, betanin; R, rutin; Q, quercetin; K, kaempferol. $^{\#}$($p < 0.05$) compared to the control group, and *($p < 0.05$) compared to blue light (BL)-induced cells alone. Data are presented by means ± SD (n = 3).

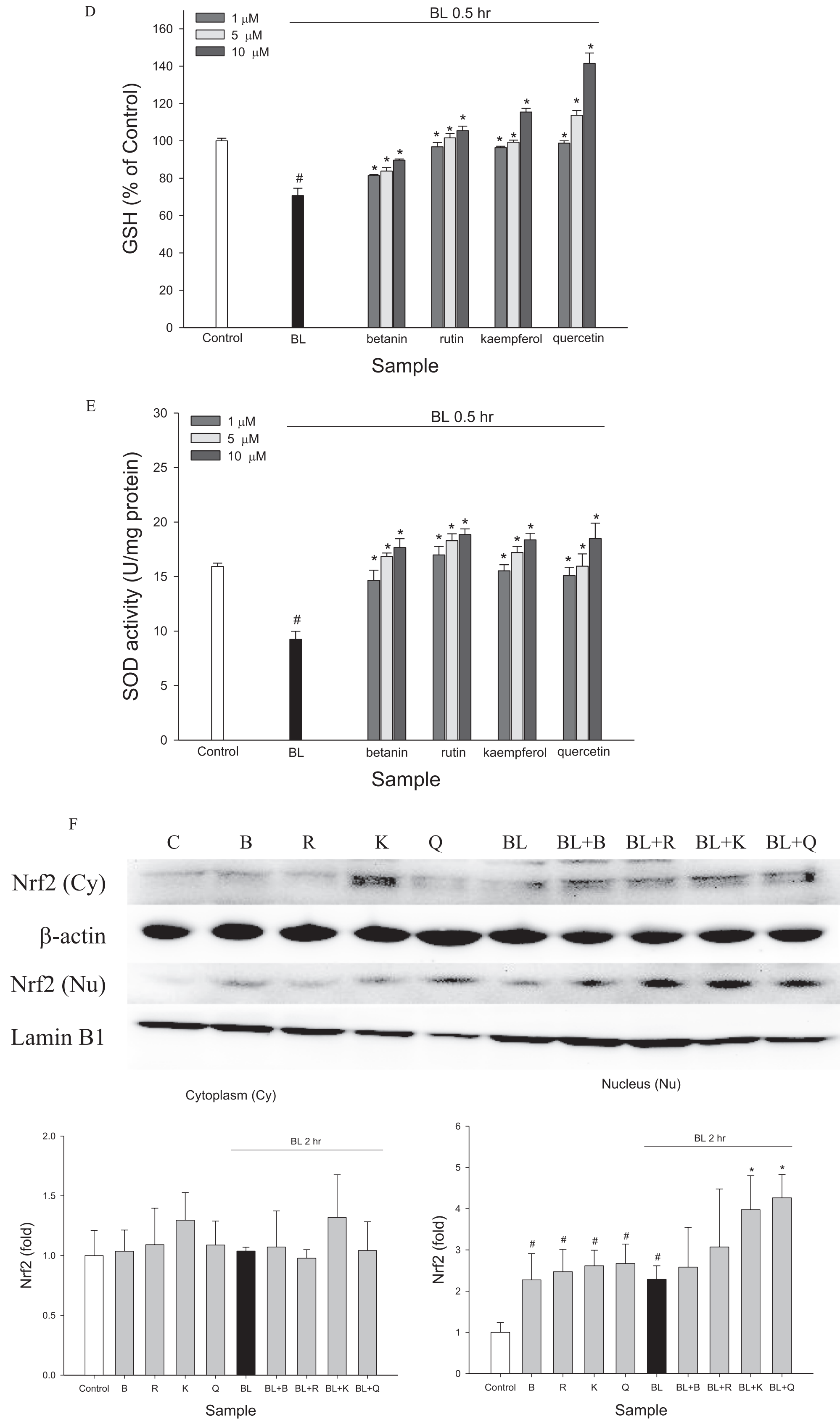

Fig. 6. (*continued*).

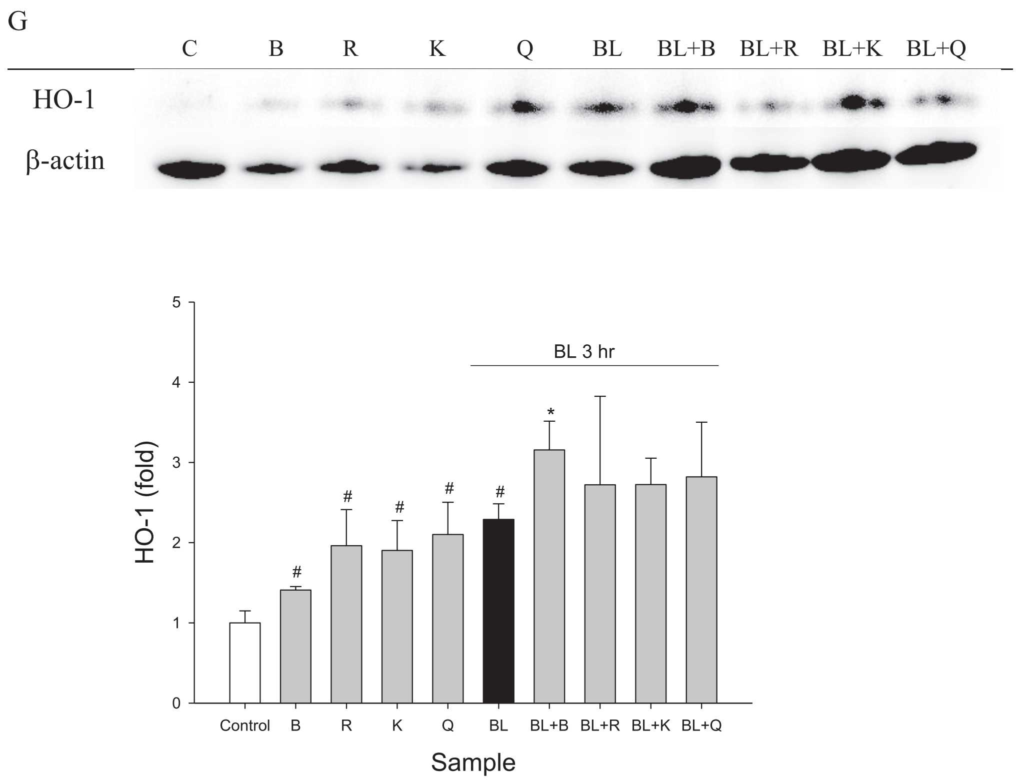

Fig. 6. (*continued*).

However, there were no significant differences among the cells treated with betanin, rutin at 1 μM and BL alone. Additionally, exposure of ARPE-19 cells to betanin, rutin, kaempferol and quercetin at concentrations ranging from 1 to 10 μM resulted in a concentration-dependent decrease in the levels of ROS production (Fig. 6B), and TBARS formation (Fig. 6C), and an increase in GSH levels (Fig. 6D) and SOD activity (Fig. 6E) in a concentration-dependent manner compared to the untreated cells. Clearly, these results indicate that photo-oxidation in BL-induced ARPE-19 cells was inhibited by betanin, rutin, kaempferol and quercetin, which could partly account for anti-photo-oxidative effect of WECF. Furthermore, the expression of Nrf2 proton in nucleus was higher in the presence of kaempferol and quercetin at 10 μM compared to BL irradiation alone, while betanin and rutin at 10 μM increased Nrf2 expression in nucleus compared to BL alone (Fig. 6F). However, there were no significant differences in Nrf2 expression between the cells treated with betanin, rutin, and BL alone. The expression of HO-1was significantly increased by betanin at 10 μM in BL-induced cells compared to BL alone (Fig. 6G). Although rutin, kaempferol, and quercetin at 10 μM also increased HO-1 expression in BL-induced cells compared to BL alone, there were no significant differences between the cells treated with these compounds and those treated with BL alone.

4. Discussion

Many naturally occurring antioxidant compounds, such as plant phytochemicals, have been shown to effectively inhibit oxidative damage (Hollman & Katan, 1999). Therefore, early nutritional and dietary intervention can be a safe and cost-effective approach to prevent and control photo-oxidative eye damage and retinal cell degeneration (Lu et al., 2016). The study aims to evaluate the anti-photo-oxidative effect and mechanism of WECF and its bioactive compounds on ARPE-19 cells, which are prone to oxidative damage due to continual exposure to BL (Lu et al., 2016).

To determine the safe concentration range of WECF that does not damage cells, cell viability was measured after treating ARPE-19 cells with WECF at concentrations ranging from 0.1 to 25 μg/mL. The results showed that cell viability above 100% was observed when the cells were treated with WECF at 0.1–25 μg/mL, indicating that WECF at the tested concentration range did not exert any cytotoxicity in ARPE-19 cells. Therefore, WECF within the range from 0.1 to 25 μg/mL was used in this study.

Exposure of the ARPE-19 cells to BL irradiation caused cell death, reduction of GSH levels, mitochondrial membrane potential and SOD activity. Furthermore, ROS production, TBARS formation and caspasen-3 activity in the cells increased under BL irradiation. Our findings confirm that excessive BL induces photo-oxidative stress, resulting in the formation of oxidation products and suppressing cellular antioxidants, such as GSH and SOD enzyme. These results are consistent with previous studies, such as that by Lee et al. (2014), who reported that overexposure to BL may have harmful effects on human corneal epithelial cells.

It is widely known that BL can participate in the generation of ROS, leading to occurrence of oxidative stress which it is phototoxic to RPE cells (Lee et al, 2014). In the present study, the results demonstrated that BL exposure decreased the viability of ARPE-19 cells and induced significant ROS production after irradiation. These findings confirm that BL has a negative impact on human eyes. Therefore, inhibiting ROS production by natural biological sources, both exogenous and endogenous, may be an effective and useful therapy for preventing photo-oxidative damage induced by BL. As expected, treatment with WECF resulted in a remarkable decrease in ROS production in BL-induced cells. Furthermore, exposure of ARPE-19 cells to BL caused a significant increase in ROS production, leading to increased lipid peroxidation and accumulation of lipid peroxides, which altered membrane fluidity and permeability. As a result, this led to the photo-toxicity of the ARPE-19 cells due to the disruption of membrane structure and biofunction (Sohn, Han, Choo, & Hwang, 2007). Therefore, the protective effect of WECF on BL-induced ARPE-19 cell death is at least partly attributed to its suppression of ROS production, thereby inhibiting photo-oxidative damage of ARPE-19 cells.

Glutathione (GSH) is a ubiquitous tripeptide, playing a crucial role in regulating cell proliferation, cell death and antioxidant through the mediation of the main redox regulatory signaling pathway in the cells (Kwon et al, 2019). However, GSH deficiency associated with oxidative stress is linked to the onset and progression of various diseases and aging. Fig. 2C shows that GSH levels in BL-induced ARPE-19 cells were significantly lower than the control, likely due to GSH reacting with free radicals and ROS generated by BL, leading to a decrease in GSH concentration (Chu, Chen, Chyan, Fu, Lin, & Duh, 2016). As expected, WECF restored GSH levels in BL-induced ARPE-19 cells in a concentration-dependent manner. At 25 μg/mL, WECF remarkably increased GSH levels to a level comparable to that of untreated cells. These results suggest that increased GSH levels in the presence of WECF enhanced the scavenging activity of free radicals and ROS, leading to an anti-photo-oxidative effect in BL-induced ARPE-19 calls.

GSH biosynthesis involves two consecutive ATP-consuming reactions from three amino acids, namely L-glutamic acid, L-cysteine, and glycine. The first reaction, catalyzed by r-glutamylcysteine synthetase (r-GCS), involves L-glutamic acid and L-cysteine to form r-glutamylcysteine (r-GC). The second reaction, catalyzed by glutathione synthetase (GS), involves r-GC and glycine to form GSH. On the other hand, glutathione reductase (GR) catalyzes the reduction of glutathione disulfide (GSSG) to the sulfhydryl form glutathione (GSH). Thus, GSH levels are regulated by r-GCS, GS and GR. Therefore, treatment that upregulates the expression of r-GCS, GS or GR may increase intracellular GSH levels (Chen, Chyau, Chu, Chen, Chen, & Duh, 2013). The r-GCS consists of a catalytic heavy subunit (r-GCS-HS) and a regulatory light subunit (r-GCS-LS) (Huang, Chang, Anderson, & Meister, 1993). Phenolic antioxidants like β-naphthoflavone increase GSH levels by inducing r-GCS-HS, and the promoter region of the r-GCS-HS gene is regulated by the active protein-1 (AP-1) binding site (Rahman & MacNee, 2000; Park, Nam, Lee, Jun, Hendrich, & Lee, 2010). Although this work did not investigate the regulation of r-GCS, GS, and GR, we hypothesize that some bioactive compounds in WECF may interact with antioxidant response elements (AREs), resulting in an increase in r-GCS, GS and GR, which could explain the increased recovery in GSH levels in BL-induced cells treated with WECF.

Superoxide anion is a ROS which is produced as a byproduct of normal metabolism. Once superabundant amounts of superoxide anion generation, it may lead to various diseases, such as stroke, inflammation, atherosclerosis, diabetes and liver disorder (Zeng, Zhang, Hu, pan, & Gong, 2019). Meanwhile, superoxide dismutase (SOD) is an antioxidant enzyme present in all aerobic cells and is considered the first line of main antioxidant defense against superoxide anion (Hou, Zhao, Wong, & Line, 2019). Superoxide anion, hydrogen peroxide (H_2O_2), and hydroxyl radicals (•OH) are the most common ROS that organisms need to cope with. SOD dismutases superoxide anion into H_2O_2 with the release of O_2, which can diffuse through aquaporins in the membranes. (Stephenie, Chang, Gnanasekaran, Zsa, & Gnanara, 2020). Furthermore, superoxide anion reacts with Cu (I), given H_2O_2 which then reacts with metal ions using Fronton reaction to form other more harmful species, such as hydroxyl radical (•OH), which accumulate ROS, and induce oxidative stress, ultimately causing to cell damage (Chu, Chen, Chyan, Wu, Chu, & Duh, 2020; Qian et al., 2009). Therefore, SOD plays an important role in countering the initial stage of ROS in singlet oxygen form and free radicals (Stephenie et al., 2020). Thus, due to antioxidant activity of SOD, it is necessary to determine whether WECF is responsible for increasing SOD activity in BL-induced ARPE-19 cells to explain the observed anti-photo-oxidative effect of WECF. Fig. 2D shows that SOD activity decreased significantly in BL-induced ARPE-19 cells, while WECF treatment concentration-dependently increased SOD activity compared to the cells treated with BL alone. This finding demonstrated that WECF, at the tested concentrations, effectively restores the BL-induced SOD activity in cells, thus reinforcing the cells to prevent BL-induced photo-oxidative damage.

Accumulating evidence suggests that accelerating ROS generation to overcome antioxidant defense systems can promote oxidative injury and lead to cell apoptosis (Chyau et al., 2015). Apoptosis is accompanied with signs of mitochondrial dysfunction, such as a loss of inner mitochondrial transmembrane potential and the release of cytochrome *c* (Chen, Chu, Chyau, Chu, & Duh, 2012; Park et al., 2003). In Fig. 3A, it can be seen that BL irradiation reduced the mitochondrial membrane potential, which was accompanied by increased ROS production and inhibited survival of ARPE-19 cell growth, indicating that BL exposure triggered apoptosis. However, treatment with WECF significantly increased the mitochondrial membrane potential compared to cells induced by BL alone, suggesting that WECF suppressed the apoptosis of BL-induced ARPE-19 cells.

Apoptosis is closely linked to oxidative stress, and caspase is a major executor of apoptotic programming. Once caspase-3 is activated, it might cause to DNA fragmentation (Park et al., 2003). In other words, caspase activation is the initiating trigger of the apoptosis pathway (Chen et al., 2012). In the current study, the effect of WECF on caspase-3 activity in BL-induced ARPE-19 cells was determined. As shown in Fig. 3B, treatment of cells with BL irradiation for 4 h significantly increased the activity of caspase-3, compared to the control. This observation suggests that the BL-induced increase in oxidative stress is associated with increased caspase-3 activity, supporting the role of caspase-3 in BL-induced apoptosis (Chen et al., 2012). However, WECF treatment resulted in a significant decrease in caspase-3 activity when compared to cells treated with BL alone. This suggests that WECF repressed apoptosis, by inhibiting the BL-induced caspase-3 activity. This finding indicates that down-regulation of caspase-3 activity is a major factor that contributes to the induction of anti-apoptosis by WECF. Thus, WECF can prevent oxidative damage caused by oxidative stress, which is generated by BL, and suppress caspase-3 activity. This observation supports the idea that the cytoprotective effect of WECF on BL-induced *in vitro* ARPE-19 cell death may be attributed, in part, to the suppression of apoptosis of ARPE-19 cells (Chyau et al., 2015). In addition, DAPI staining is commonly used to study the morphological changes in nuclei of cells. The DAPI results in the present work showed that the apoptotic cells were predominantly seen in BL-induced cells. However, WECF treatment results in less fragmentation in the chromatin and DNA rings within the nucleus of the treated cells, which is indicative of anti-apoptosis. Moreover, the results showed that the increase of mitochondrial membrane potential (Fig. 3A) was parallel to the inhibition of caspase-3 activity (Fig. 3B), as well as the DAPI staining results (Fig. 3C). Herein, these observations support the conclusion that WECF promotes anti-apoptosis in BL-induced ARPE-19 cells in a dose-dependent manner (Chyau et al., 2015).

To elucidate the mechanism action underlying the anti-photo-oxidative effect of WECF, the effects of WECF on the NF-κB and MAPK signaling pathways were further investigated. The results showed that the BL treatment significantly increased the nuclear protein level of NF-κB (Fig. 4A) compared with that in untreated controls, confirming the activation of the NF-κB pathway (Li, Dong, Du, Bao, & Lin, 2021). However, WECF significantly inhibited the activation of NF-κB to nucleus compared to the cells treated with BL alone. Different models of oxidative stress can both activate and repress NF-κB signaling in a phase and context-dependent manner. Moreover, the NF-κB pathway can have both anti- and pro-oxidant roles in the setting of oxidative stress (Lingappan, 2018). BL-induced ROS production promotes NF-κB phosphorylation and subsequent the nuclear translocation of NF-κB, leading to ARPE-19 cell damage (Kuse, Ogawa, Tsuruma, Shimazawa, & Hara, 2014). In the present work, WECF suppressed NF-κB phosphorylation, the nuclear translocation of NF-κB, and ROS generation induced by BL irradiation in ARPE-19 cells. Therefore, it can be suggested that WECF attenuated BL-induced photo-oxidative damage in ARPE-19 cells, in part due to inhibition of NF-κB signaling pathway.

To clarify the intracellular molecular mechanisms underlying the protective effect of WECF on photo-oxidative stress, we evaluated the influence of WECF on MAPK signaling pathways, which are closely related to oxidative stress. The data shown in Fig. 4B demonstrated that BL treatment alone significantly enhanced the phosphorylation of JNK, ERK, and p38 in ARPE-19 cells, while WECF treatment suppressed BL-induced phosphorylation of these MAPKs. It is well known that MAPK family consists of serine/threonine kinases that form a ubiquitous transduction system controlling cell proliferation, differentiation, survival, and apoptosis (Pocrnich, et al., 2009). The distinct sub-families of MAPK include the extracellular signal-regulated kinases (ERK), the c-Jun NH2-terminal kinases (JNK), and p38 kinases. Several studies have noted that MAPKs are activated by ROS generated intracellularly (Kulisz, Chen, Chandel, Shao, & Schumacker, 2002). However, studies of oxidant-induced activation of MAPK pathway have also provided conflicting results (Pocrnich et al., 2009). For instance, in response to environmentally induced oxidative stresses, p38 MAPK induces RPE cell death, while in other studies using the same ARPE-19 cell line, p38 MAPK has been reported to protect RPE cells from oxidative damage (Wang, 2014). In other words, the influence of MAPK activation on cell survival in the face of an oxidative change is not clear-cut (Pocrnich et al., 2009). As shown in Fig. 4B, BL activated the ERK, JNK, and p38 signaling pathways. As expected, the increased phosphorylation of ERK, JNK, and p38 were reversed in the presence of WECF, indicating that ERK, JNK, and p38 pathways may be involved in BL-induced ROS-mediated ARPE-19 cells death. Interestingly, the results obtained supported a protective role of WECF in ARPE-19 cells exposed to BL challenge, at least in part, through inhibition of the phosphorylation of MAPKs, thereby blocking the MAPK signaling pathways.

Nrf2 pathway is an important cellular defense mechanism that regulates the expression of many antioxidant genes, including phase 2 antioxidant enzymes, such as HO-1 and GST, to maintain intracellular redox homeostasis (Lu et al., 2016). Several studies have reported that the MAPK signaling pathway activates Nrf2 (Banerjee, Basu, Datta, Gasser, Wanga-Gasser, & Pal, 2011; Lu et al., 2016). For instance, the ERK1/2 and p38 MAPK pathways may up-regulate Nrf2 transcription activity (Do et al., 2013; Wang, Li, Li, Wang, & Li, 2020). Consistent with these studies, Fig. 4B indicates that BL actives the MAPK signaling pathways, thereby up-regulating Nrf2 transcription activity (Fig. 5A). The findings are consistent with a previous study that show Nrf2 gene expression increased with BL exposure (Suárez-Barrio et al., 2020). Meanwhile, the results also show that under the BL stimulation, nuclear Nrf2 and HO-1 expression increase, as a cell-protective response to ROS. However, photo-oxidative damage still occurs in cells, suggested that Nrf2 activation is not sufficient to resist photo-oxidative damage caused by oxidative stress (Wang et al., 2000). Moreover, accumulating evidence shows that naturally occurring antioxidant compounds can protect cells from oxidative stress injury by up-regulating antioxidant enzymes, such as HO-1, that are regulated by Nrf2 signaling pathway (Xiong, Li, Yao, Xu, & Wang, 2022). To clarify whether WECF mediated Nrf2 gene expression in BL-induced ARPE-19 cells, a Western blot analysis of both cytoplasmic and nuclear Nrf2 fractions was performed. As shown in Fig. 5A, cytoplasmic Nrf2 expression in the presence of WECF plus BL treatment or in BL treatment alone decreased compared to the control. However, after treatment with WECF, the expression of Nrf2 in the nucleus significantly increased compared to the control. Many studies have reported that Nrf2 can combine with antioxidant response elements (ARE), which include encoding of antioxidant enzymes (Xiong, et al., 2022). When cells are attacked by oxidative stress, Nrf2 may transfer to nucleus and activate the transcription of these antioxidant enzymes. Furthermore, the difference in Nrf2 protein expression between the cytoplasm and nucleus reveals that WECF activated Nrf2 transfer to the nucleus (Xiong et al., 2022). In addition, the protein levels of HO-1 were measured using immunoblotting. The results show that HO-1 gene expression significantly increased with BL compared to the control. However, WECF, in the presence of BL, caused an even greater increase, which could be explained by the increased in nucleus, indicating that WECF successfully activated the Nrf2/HO-1 signaling pathway. As a result, WECF stimulates the antioxidant pathway in BL-induced ARPE-19 cells (Wang et al., 2020; Suárez-Barrio et al., 2020). Therefore, WECF may act as an activator of the Nrf2/ARE signaling pathway. Taken together, WECF has been observed to decrease ROS production (Fig. 2A) and TBARS formation (Fig. 2B), restore GSH levels (Fig. 2C), enhance SOD activity (Fig. 2D), and trigger the Nrf2/HO-1 signaling pathway (Fig. 5A and 5B) in BL-induced cells. This sequence of events inhibits photo-oxidative stress and consequently mitigates cell death caused by BL irradiation.

Naturally occurring bioactive compounds from natural sources have been found to have multifunctional activity against oxidative stress, inflammation, and other human diseases (Chu et al., 2016). As a result, natural biological compounds have gained attention in research for natural bioactive compounds that contribute to anti-photo-oxidative activity (Suárez-Barrio et al., 2020). In previous studies by the authors reported that betanin, rutin, quercetin, kaempferol and other compounds were identified and found to be present in WECF (Chu et al., 2022). The percentages of betanin, kaempferol, quercetin, and rutin in WECF were 0.0589%, 0.0212%, 0.2648%, and 0.2219%, respectively (Chu et al., 2022). Given the presence of bioactive compounds in WECF, these compounds may have biological activities and play a critical role in preventing or inhibiting photo-oxidative damage in BL-induced cells. Therefore, it is necessary to investigate whether the bioactive compounds, such as betanin, rutin, quercetin and kaempferol, identified in WECF were responsible for protecting BL-induced ARPE-19 cells from photo-oxidative stress. The effects of bioactive compounds on the growth of ARPE-19 cells, ROS production, TBARS formation, GSH restoration, SOD activity, Nrf2 protein expression, and HO-1 protein levels in BL-induced cells were further examined. As expected, treatment of ARPE-19 cells with betanin, rutin, quercetin, and kaempferol at 1–10 μM showed no cytotoxicity effect on ARPE-19 cell growth. Moreover, treatment of ARPE-19 cells with these bioactive compounds at 1–10 μM significantly protected cells from BL-induced cytotoxicity (Fig. 6A), indicating the protective effect of betanin, rutin, quercetin and kaempferol against BL-induced photo-toxicity. Additionally, the results showed that betanin, rutin, quercetin and kaempferol at 1–10 μM significantly decreased ROS production (Fig. 6B) and TBARS formation (Fig. 6C), restored GSH levels (Fig. 6D) and increased SOD activity (Fig. 6E), Nrf2 protein expression (Fig. 6F), and HO-l protein levels (Fig. 6G) in BL-induced ARPE-19 calls. These observations suggest that cytoprotective effect of WECF on BL-induced ARPE-19 cells *in vitro* cell death may be partly attributable to the antioxidant potential and suppression of oxidative damage of the cells treated with bioactive compounds, such as betanin, rutin, quercetin and kaempferol. In addition, previous studies by the authors showed that other identified compounds and uncharacterized compounds were present in WECF (Chu et al., 2022). Many studies have proposed that synergistic effects of phytochemicals in plants account for their remarkable antioxidant and anticancer activity, which gives significant meaning to the use of natural antioxidants for chemoprevention or therapy for human diseases (Blasa, Angelino, Gennari, & Ninfali, 2011). Therefore, it is speculated that the bioactive compounds present in WECF may be the result of synergistic effects between compounds, which may explain why WECF protects, at least in part, against photo-oxidative stress in BL-induced ARPE-19 cells.

5. Conclusion

This study demonstrated that supplementation with djulis may protect RPE cells from photo-oxidative injury induced by blue light by reversing the increase in oxidative stress, restoring enzymatic and non-enzymatic antioxidants via suppressing NF-κB and MAPK signaling, and activating the Nrf2/HO-1 pathways. These results suggest that djulis, which is rich in bioactive compounds such as betanin, rutin, quercetin, and kaempferol, may be a potentially suitable candidate for therapeutic effects on RPE disorders caused by photo-oxidative damage. Further *in vivo* studies are currently being conducted to verify the anti-photo-oxidative effect of WECF.

CRediT authorship contribution statement

Ching-Chih Liu: Conceptualization, Investigation, Methodology, Resources. **Chin-Chen Chu:** Investigation, Conceptualization, Methodology. **Shih-Ying Chen:** Investigation, Formal analysis. **Ying-Chun Lin:** Investigation. **Pin-Der Duh:** Writing – review & editing, Writing – original draft, Visualization, Validation, Supervision, Resources, Project administration, Methodology, Investigation, Funding acquisition, Formal analysis, Data curation, Conceptualization.

Declaration of Competing Interest

The authors declare the following financial interests/personal relationships which may be considered as potential competing interests: Pin-Der Duh reports equipment, drugs, or supplies and travel were provided by Ministry of Science and Technology of the Republic of China. Pin-Der Duh reports equipment, drugs, or supplies and travel were provided by Ministry of Science and Technology of the Republic of China. Pin-Der Duh reports a relationship with Ministry of Science and Technology of the Republic of China that includes: funding grants and travel reimbursement. Pin-Der Duh has patent pending to no. All the authors have not served any editorial capacity for this Journal.

Data availability

Data will be made available on request.

Acknowledgement

This research work was supported by research grants from the Ministry of Science and Technology of the Republic of China (MOST 110-2320-B-041-001MY2).

References

Banerjee, P., Basu, A., Datta, D., Gasser, M., Waaga-Gasser, A. M., & Pal, S. (2011). The heme oxygenase-1 protein is overexpressed in human renal cancer cells following activation of the Ras-Raf-ERK pathway and mediates anti-apoptotic signal. *Journal of Biological Chemistry, 286*, 33580–33590. https://doi.org/10.1074/jbc.M111.248401

Blasa, M., Angelino, D., Gennari, L., & Ninfali, P. (2011). The cellular antioxidant activity in red blood cells (CAA-RBC): A new approach to bioavailability and synergy of phytochemicals and botanical extracts. *Food Chemistry, 125*, 685–691. https://doi.org/10.1016/j.foodchem.2010.09.065

Chen, S. Y., Chu, C. C., Chyau, C. C., Fu, Z. H., & Duh, P. D. (2018). Effect of water extract of djulis *(Chenopodium formosaneu*m) and its bioactive compounds on alcohol-induced liver damage in rats. *International Journal of Food and Nutritional Science, 5* (1), 55–63. https://doi.org/10.15436/2377-0619.18.1816

Chen, S. Y., Chu, C. C., Chyau, C. C., Yang, J. W., & Duh, P. D. (2019). Djulis *(Chenopodium formosanu*m) and its bioactive compounds affect vasodilation, angiotensin converting enzyme activity, and hypertension. *Food Bioscience, 32*, Article 100469. https://doi.org/10.1016/j.fbio.2019.100469

Chen, S. Y., Chu, C. C., Lin, Y. C., & Duh, P. D. (2019). Djulis *(Chenopodium formosanu*m) and its bioactive compounds for management of hyperlipidemia and hyperglycemia in high-fat diet-fed mice. *Journal of Food and Nutrition Research, 7*(6), 452–457. https://doi.org/10.12691/jfnr-7-6-7

Chen, S. Y., Chyau, C. C., Chu, C. C., Chen, Y. H., & Duh, P. D. (2013). Hepatoprotection using sweet orange peel and its bioactive compound, hesperidin, for CCl4-induced liver injury in vivo. *Journal of Functional Foods, 5*, 1591–1600. https://doi.org/10.1016/j.jff.2013.07.001

Chen, Z. T., Chu, H. L., Chyan, C. C., Chu, C. C., & Duh, P. D. (2012). Protective effects of sweet orange (*Citrus sinensis*) peel and their bioactive compounds on oxidative stress. *Food Chemistry, 135*, 2119–2127. https://doi.org/10.1016/j.foodchem.2012.07.041

Chirico, S., Smith, C., Marchant, C., Mitchinson, M. J., & Halliwell, B. (1993). Lipid peroxidation in hyperlipidaemic patients. A study of plasma using an HPLC-based thiobarbituric acid test. *Free Radical Research Communications, 19*, 51–57.

Chu, C. C., Chen, S. Y., Chyau, C. C., Fu, Z. H., Liu, C. C., & Duh, P. D. (2016). Protective effect of Djulis (Chenopodium formosaneum) and its bioactive compounds protect against carbon tetrachloride-induced liver injury, in vivo. *Journal of Functional Foods, 26*, 585–597.

Chu, C. C., Chen, S. Y., Chyau, C. C., Wang, S. C., Chu, H. L., & Duh, P. D. (2022). Djulis *(Chenopodium formosanu*m) and Its Bioactive Compounds Protect Human Lung Epithelial A549 Cells from Oxidative Injury Induced by Particulate Matter via Nrf2 Signaling Pathway. *Molecules, 27*, 253. https://doi.org/10.3390/molecules27010253

Chu, C. C., Chen, S. Y., Chyau, C. C., Wu, Y. C., Chu, H. L., & Duh, P. D. (2020). Anticancer activity and mediation of apoptosis in hepatoma carcinoma cells induced by djulis and its bioactive compounds. *Journal of Functional Foods, 75*, Article 104225.

Chyau, C. C., Chu, C. C., Chen, S. Y., & Duh, P. D. (2015). Djulis *(Chenopodium formosaneu*m) and its bioactive compounds protect against oxidative stress in human HepG2 cells. *Journal of Functional Foods, 18*, 159–170. https://doi.org/10.1016/j.jff.2015.0

Chyau, C. C., Chu, C. C., Chen, S. Y., & Duh, P. D. (2018). The Inhibitory effects of Djulis (Chenopodium formosanum) and its bioactive compounds on adipogenesis in 3T3-L1 adipocytes. *Molecules, 23*, 1780. doi:0.3390.

Do, M. T., Kim, H. G., Khanal, T., Choi, J. H., Kim, D. H., Jeong, T. C., & Jeong, H. G. (2013). Metformin inhibits heme oxygenase-1 expression in cancer cells through inactivation of Raf-ERK-Nrf2 signaling and AMPK-independent pathways. *Toxicology and Applied Pharmacology, 271*, 229–238. https://doi.org/10.1016/j.taap.2013.05.010

Duh, P. D., Chen, Z. T., Lee, S. W., Lin, T. P., Wang, Y. T., Yen, W., … Chu, H. L. (2012). Antiproliferative activity and apoptosis induction of Eucalyptus citriodora resin and its major bioactive compound in melanoma B16F10 cells. *Journal of Agricultural and Food Chemistry, 60*, 7866–7872. http://refhub.elsevier.com/S1756-4646(15)00319-9/sr0050.

Hollman, P. C. H., & Katan, M. B. (1999). Dietary Flavonoids: Intake, Health Effects and Bioavailability. *Food and Chemical Toxicology, 37*, 937–942. https://doi.org/10.1016/S0278-6915(99)00079-4

Hong, Y. H., Huang, Y. L., Liu, Y. C., & Tsai, P. J. (2016). Djulis *(Chenopodium formosanu*m Koidz.) Water Extract and Its Bioactive Components Ameliorate Dermal Damage in UVB-Irradiated Skin Models. *BioMed Research International, 2016*, 7368797. https://doi.org/10.1155/2016/7368797

Hou, Z., Zhao, L., Wang, Y., & Liao, X. (2019). Effects of high pressure on activities and properties of superoxide dismutase from chestnut rose. *Food Chemistry, 294*, 557–564. https://doi.org/10.1016/j.foodchem.2019.05.080

Huang, C. S., Chang, L. S., Anderson, M. E., & Meister, A. (1993). Catalytic and regulatory properties of the heavy subunit of rat kidney gammaglutamylcysteine synthetase. *Journal of Biological Chemistry, 268*(26), 19675–19680.

Kuse, Y., Ogawa, K., Tsuruma, K., Shimazawa, M., & Hara, H. (2014). Damage of photoreceptor-derived cells in culture induced by light emitting diode-derived blue light. *Scientific Reports, 9*(4), 5223. https://doi.org/10.1038/srep05223

Kulisz, A., Chen, N., Chandel, N., Shao, Z., & Schumacker, P. T. (2002). Mitochondrial ROS initiate phosphorylation of p38 MAPkinase during hypoxia in cardiomyocytes. *American Journal of Physiology Lung Cellular and Molecular Physiology., 282*, L1324–L1329. https://doi.org/10.1152/ajplung.00326.2001

Kwon, D. H., Cha, H. J., Lee, H., Hong, S. H., Park, C., Park, S. H., & Choi, Y. H. (2019). Protective Effect of Glutathione against Oxidative Stress-induced Cytotoxicity in RAW 264.7 Macrophages through Activating the Nuclear Factor Erythroid 2-Related Factor-2/Heme Oxygenase-1 Pathway. *Antioxidants, 8*(82). https://doi.org/10.3390/antiox8040082

Lee, C. W., Chen, H. J., Xie, G. R., & Shih, C. K. (2019). Djulis *(Chenopodium Formosanu*m) prevents colon carcinogenesis via regulating antioxidative and apoptotic pathways in rats. *Nutrients, 11*, 2168. https://doi.org/10.3390/nu11092168

Lee, J. B., Kim, S. H., Lee, S. C., Kim, H. G., Ahn, H. G., Li, Z., & Yoon, K. C. (2014). Blue light–induced oxidative stress in human corneal epithelial cells: Protective effects of ethanol extracts of various medicinal plant mixtures. *Investigative Ophthalmology & Visual Science, 55*, 4119–4127. https://doi.org/10.1167/iovs.13-13441

Lingappan, K. (2018). NF-κB in Oxidative Stress. *Current Opinion in Toxicology, 7*, 81–86. https://doi.org/10.1016%2Fj.cotox.2017.11.002.

Lu, B., Sun, T., Li, W., Sun, X., Yao, X., & Sun, X. (2016). Piceatannol protects ARPE-19 cells against vitamin A dimer-mediated photo-oxidative damage through activation of Nrf2/NQO1 signalling. *Journal of Functional Foods, 26*, 739–749. https://doi.org/10.1016/j.jff.2016.08

Li, M., Dong, L., Du, H., Bao, Z., & Lin, S. (2021). Potential mechanisms underlying the protective effects of Tricholoma matsutake singer peptides against LPS-induced inflammation in RAW264.7 macrophages. *Food Chemistry, 353*. https://doi.org/10.1016/j.foodchem.2021.129452

Ness, A. R., & Powles, J. W. (1997). Fruit and vegetables, and cardiovascular disease: A review. *International Journal of Epidemiology, 26*, 1–13. http://refhub.elsevier.com/S1756-4646(16)30239-0/sr0115.

Park, C., So, H. S., Shin, C. H., Baek, S. H., Moon, B. S., & Shin, S. H. (2003). Quercetin protects the hydrogen peroxide induced apoptosis via inhibition of mitochondrial dysfunction in H9c2 cardiomyoblast cell. *Biochemical Pharmacology, 66*, 1287–1295. https://doi.org/10.1016/s0006-2952(03)00478-7

Park, H. Y., Nama, M. H., Lee, H. S., Jun, W., Hendrich, S., & Lee, K. W. (2010). Isolation of caffeic acid from Perilla frutescens and its role in enhancing c-glutamylcysteine synthetase activity and glutathione level. *Food Chemistry, 119*, 724–730. https://doi.org/10.1016/j.foodchem.2009.07.020

Pocrnich, C. E., Liu, H., Feng, M., Peng, T., Feng, O., & Hutnik, C. M. L. (2009). p38 mitogen-activated protein kinase protects human retinal pigment epithelial cells exposed to oxidative stress. *Canadian Journal of Ophthalmology, 44*, 431–436. https://doi.org/10.3129/i09-109

Qian, Y. P., Cai, Y. J., Fan, G. J., Wei, Q. Y., Yang, J., Zheng, L. F., & Zhou, B. (2009). Antioxidant-based lead discovery for cancer chemoprevention: The case of resveratrol. *Journal of Medicinal Chemistry, 52*, 1963–1974. https://doi.org/10.1021/jm80154

Rahman, I., & MacNee, W. (2000). Oxidative stress and regulation of glutathione in lung inflammation. *European Respiratory Journal, 3*, 534–554.

Sohn, J. H., Han, K. L., Choo, J. H., & Hwang, J. K. (2007). Macelignan protects HepG2 cells against tert-butylhydroperoxide-induced oxidative damage. *BioFactor, 29*, 1–10. https://doi.org/10.1002/biof.5520290101

Stephenie, S., Chang, Y. P., Gnanasekaran, A., Esa, N. M., & Gnanaraj, C. (2020). An insight on superoxide dismutase (SOD) from plants for mammalian health enhancement. *Journal of Functional Foods, 68*, Article 103917. https://doi.org/10.1016/j.jff.2020.103917

Suárez-Barrio, C., Olmo-Aguado, S., García-Pérez, E., Fuente, M., Muruzabal, F., Anitua, E., & Merayo-Lloves, J. (2020). Antioxidant Role of PRGF on RPE Cells after Blue Light Insult as a Therapy for Neurodegenerative Diseases. *International Journal of Molecular Sciences, 21*, 1021. https://doi.org/10.3390/ijms21031021

Tsuchida, K., & Sakiyama, N. (2023). Blue light–induced lipid oxidation and the antioxidant property of hypotaurine: Evaluation via measuring ultraweak photon emission. *Photochemical & Photobiological Sciences, 22*, 345–356. https://doi.org/10.1007/s43630-022-00319-8

Wang, H., & Joseph, J. A. (1999). Quantifying cellular oxidative stress by dichlorofluorescein assay using microplate reader. *Free Radical Biology and Medicine, 27*, 612–616. https://doi.org/10.1016/S0891-5849(99)00107-0

Wang, Y., Li, C., Li, J., Wang, G., & Li, L. (2020). Non-esterified Fatty Acid-Induced Reactive Oxygen Species Mediated Granulosa Cells Apoptosis Is Regulated by Nrf2/p53 Signaling Pathway. *Antioxidants, 9*(6), 523. https://www.mdpi.com/2076-3921/9/6/523.

Wang, Z. (2014). MAPKs Modulate RPE Response to Oxidative Stress. *Journal of Medical and Bioengineering, 3*(1), 67–72.

Wu, M. J., Huang, C. J., Lian, T. W., Kou, M. C., & Wang, L. S. (2005). Antioxidant activity of *Glossogyne tenuifolia*. *Journal of Agricultural and Food Chemistry, 53*(16), 6305–6312. https://doi.org/10.1021/jf050511a

Xiong, W., Li, Y., Yao, Y., Xu, Q., & Wang, L. (2022). Antioxidant mechanism of a newly found phenolic compound from adlay (NDPS) in HepG2 cells via Nrf2 signalling. *Food Chemistry, 378*, Article 132034. https://doi.org/10.1016/j.foodchem.2021.132034

Yen, W. J., Chyau, C. C., Lee, C. P., Chu, H. L., Chang, L. W., & Duh, P. D. (2013). Cytoprotective effect of white tea against H2O2-induced oxidative stress in vitro. *Food Chemistry, 141*, 4107–4114. https://doi.org/10.1016/j.foodchem.2013.06.106

Zeng, N., Zhang, G., Hu, X., Pan, J., & Gong, D. (2019). Mechanism of fisetin suppressing superoxide anion and xanthine oxidase activity. *Journal of Functional Foods, 58*, 1–10. https://doi.org/10.1016/j.jff.2019.04.044